PERGAMON

European Journal of Cancer 39 (2003) 1468–1477

European Journal of Cancer

www.ejconline.com

TNF increases camptothecin-induced apoptosis by inhibition of NF-κB

P. Valente[a], D. Arzani[b,1], A. Cesario[c], S. Margaritora[c], E. Carbone[b], P. Russo[b,*]

[a]*Medical Oncology, University of Genova, Italy*

[b]*Molecular Pathology Section, Laboratory of Experimental Oncology, National Institute for Research on Cancer, Largo Rosanna Benzi 10, I-16132 Genova, Italy*

[c]*Department of Surgical Science, Division of Thoracic Surgery, Catholic University, Rome, Italy*

Received 9 December 2002; received in revised form 28 February 2003; accepted 21 March 2003

Abstract

rHuTNF potentiates CPT-cytotoxicity in human ovarian A2780 cells. In this study, we examined the role of NF-κB in this potentiation. A pulse-labelled DNA study indicated that the combination CPT + TNF had little effect on the rate of DNA elongation at 6 h after drug removal, whereas CPT alone produced a complete inhibition for at least 6 h after drug removal. Flow cytometry analyses showed that CPT + TNF arrested cells in the G_2-M phase, whereas CPT blocked cells in S phase. Looking at the persistence of the NF-κB complexes in cells, it appeared that they were still present at 24 h in TNF-treated cells. In contrast, in CPT-treated cells they persisted for 6 h. In CPT + TNF-treated cells, the NF-κB complexes disappeared quickly and became undetectable at 6 h. The induction of apoptosis was detected only in the CPT + TNF treated cells (using flow cytometry, a filter binding assay and ApopTag staining). These findings show that TNF, in combination with CPT, reduces the time that NF-κB complexes persist in cells likely resulting in the induction of apoptosis.

Keywords: Apoptosis; Camptothecin; TNF; NF-κB; DNA elongation; DNA synthesis cell cycle; Cytotoxicity; Ovarian cancer cells

1. Introduction

The transcriptor factor nuclear factor-kappaB (NF-κB) is involved not only in inflammatory diseases and in oncogenesis but also in apoptotic processes induced by cytokines and antitumour drugs [1,2]. Tumour necrosis factor (TNF), chemotherapy and radiation can activate NF-κB, and this response potently suppresses the apoptotic potential of these stimuli *in vitro* [1–6]. Although there may be many mechanisms by which resistance to apoptosis is achieved in tumours, experimental data indicate that a major pathway involved in this inducible resistance is the activation of NF-κB within tumours in response to chemotherapy or TNF [2–3,6]. In either case, inhibition of cancer therapy-induced NF-κB activation strongly enhances the apoptotic potential of these stimuli. Recently, we have shown that Human Papilloma Virus-16 (HPV-16) E6 enhances TNF-induced apoptosis by interfering with NF-κB activity in the human ovarian cancer cell line A2780 [7]. Camptothecin (CPT) is an anticancer agent that inhibits DNA Topoisomerase I (Top I) activity, causes the formation of DNA-double-strand breaks (DSB) during DNA replication [8] and activates NF-κB [3,6]. Recent studies have shown that NF-κB inhibition augments CPT-induced apoptosis [3,6]. The realisation that TNF, given simultaneously with CPT, enhances CPT-cytotoxicity in the A2780 human ovarian cancer cell line [9] led us to examine the role of NF-κB in this potentiation.

2. Materials and methods

2.1. Cell culture and drugs

The human ovarian cancer cell line, A2780, was maintained in Roswell Park Memorial Institute (RPMI) 1640 supplemented with 10% Foetal Calf Serum (not

* Corresponding author. Tel.: +39-010-5600212; fax: +39-010-5600217.

E-mail address: patrizia.russo@istge.it (P. Russo).

[1] Present address: Division of Public Health, Catholic University, Rome, Italy.

0959-8049/03/$ - see front matter © 2003 Elsevier Science Ltd. All rights reserved.
doi:10.1016/S0959-8049(03)00301-0

heat inactivated) without antibiotics. CPT was obtained from Sigma (St Louis, Mo); recombinant human (rHu)TNF was obtained from KNOLL-BASF (Ludwigshafen, Germany). A stock solution of rHuTNF, containing 0.1 mg/ml of protein was stored at −80 °C. Specific activity was 8.74×10^6 U/mg protein [1000 U/ml ≅ 1.38 ng/ml (48 h L929 bioassay without Actinomycin D, as determined in the KNOLL-BASF Laboratory)].

2.2. Cytotoxicity assay and morphological assessment

Drug-induced cytotoxicity was determined by a standard clonogenic assay (drug exposure for 1 h) as previously described in Ref. [10]. Cell colonies were counted after 10 days.

The inhibitory concentration (IC_{50}) value was calculated by linear interpolation of the values immediately higher and lower than 50% inhibition. IC_{50} values were estimated fitting the data with a non-linear regression to the dose-effect model derived by Chou and Talalay [11,12]:

$$f_a/f_u = (D/D_m)^m \quad (1)$$

where D is the dose of the drug, D_m is the IC_{50}, f_a is the fraction affected by the dose, f_u is the fraction unaffected, and m is a coefficient that determines the sigmoidicity of the curve.

Morphological assessment was determined by staining the cell with ApopTag. After cytospinning the A2780 cells to slides, the ApopTag peroxidase *in situ* apoptosis assay (catalogue No. S7100) was performed as described by the manufacturer (Intergen, Purchase, NY). The cells (1×10^4) were cytospinned to the poly-L-lysine pre-coated slides at 750*g* for 5 min. The cells were fixed in 4% paraformaldehyde for 30 min. Cells were incubated in a humidified chamber with TdT enzyme for 1 h at 37 °C (for the negative control water was used instead of TdT), then soaked in a stop-wash buffer (Intergen) for 30 min, rinsed in Phosphate-buffered saline (PBS) (three times) and finally incubated with anti-digoxigenin-peroxidase (Intergen) at room temperature in a humidified chamber for 30 min. The brown colour development was achieved by incubating for 6 min at room temperature with a substrate solution containing 0.008% 3,3′-diaminobenzidine tetra hydrochloride and 0.02% hydrogen peroxide. The slides were counterstained in a methyl green solution for 10 min and visualised and scored under a light microscope. One thousand cells were scored, randomly, per slide to evaluate dark-brown colour in the nuclei. Pictures were taken at 400× magnification.

2.3. Flow cytometry

Cells were plated in the log phase in T75 flasks (2700 cells/cm^2) in complete medium for 24 h, treated for 1 h with CPT, TNF or CPT + TNF and incubated in drug-free medium for an additional 24 h and then counted before performing flow cytometry. Samples were prepared for flow cytometry essentially as previously described in Ref. [13]. Briefly, cells were washed with 1× PBS pH 7.4 and then fixed with ice-cold 70% ethanol. Samples were washed with 1× PBS and stained with propidium iodide 60 μg/ml (Sigma, St. Louis, MO) containing RNase 2 μg/ml (Sigma, St. Louis, MO) for 30 min at 37 °C. Cell cycle analysis was performed using a Becton Dickinson Fluorescence-activated cell analyser and Cell Quest version 1.2 software (Becton Dickinson Immunocitometry Systems, Mansfield, MA). For each sample, at least 15 000 cells were analysed and quantitation of the cell cycle distribution was performed using the ModFit LT Version 1.01 software (Verity Software House Inc., Topsham, ME).

2.4. Measurement of DNA elongation by alkaline elution

DNA elongation was measured using pulse-labelling alkaline elution as previously described in Ref. [14]. Exponentially growing cells were pulse-labelled for 15 min with *methyl*-[^{3}H] thymidine (1 μCi/ml medium), washed twice in preheated PBS, and then incubated in radioactivity-free medium with CPT, TNF alone or with CPT + TNF at 37 °C. After 1 h, cells were washed twice in preheated PBS and maintained at 37 °C. Aliquots were removed after different times and analysed by alkaline elution as previously described in Refs. [14,15].

2.5. DNA synthesis inhibition

Cellular DNA of exponentially growing cells was labelled with 0.005 μCi/ml [^{14}C]thymidine (53.6 mCi/mmol) for 48 h at 37 °C. The rate of DNA synthesis was measured by 10-min pulses with 1 μCi/ml [methyl-^{3}H] thymidine (80.9 Ci/mmol). Tritiated thymidine incorporation was stopped by washing cell cultures twice in ice-cold HBSS and then scraping in 4 ml of ice-cold HBSS. One ml aliquots were transferred in Eppendorf tubes and precipitated with 100 μl of 100% trichloroacetic acid (TCA). Samples were vortexed, mixed and centrifuged for 10 min at high speed in a microfuge at 4 °C. The precipitates were dissolved overnight at 37 °C in 0.5 ml of 0.4 M NaOH. Samples were counted by dual-label liquid scintillation counting, and ^{3}H values were normalized using ^{14}C counts. Inhibition of DNA synthesis was calculated as the ratio of ^{3}H/^{14}C ratio in treated samples to ^{3}H/^{14}C in control cells.

2.6. DNA secondary fragmentation assay

Apoptosis-associated DNA fragmentation was analysed by a filter binding assay (FBA) as previously described [16]. A FBA was performed under non-deproteinizing

conditions using protein-adsorbing filters (vinyl/acrylic copolymers filters, Metricel membrane, 0.8 mm pore size, 25 mm diameter; Gelman; Sciences) according to Bertrand and Pommier [16]. Results are expressed as the percentage of DNA fragmented in treated cells compared with DNA fragmented in control untreated cells (background) using the formula:

$$[(F - F_0)/(1 - F_0)] \times 100$$

Where F and F_0 represent DNA fragmentation in treated and control cells, respectively.

2.7. Statistical analysis

Both parametric [Student's t-test (non-significant $P > 0.05$)] and non-parametric (Mann–Whitney test) statistics were used. For each drug combination, the combination index (CI) [CI < 0.3: strong synergism, CI = 1: additive, CI > 1: antagonism] and its 95% confidence interval (CI) were estimated. CI values were calculated on the basis of the calculated parameter for the dose–response function of each drug. To extrapolate confidence limits (i.e. statistical significance) for CI values, we conducted a parametric bootstrapping where we assumed the distribution of parameters (m and D_m) as formulated in Eq. (1) to be approximately gaussian with an estimated mean and asymptotic standard error as calculated using non-linear regression commands of Statistical Package for the Social Sciences (SPSS) software.

2.8. Gel mobility shift assay (EMSA)

Nucleic extracts were prepared according to the method of Scheiber and colleagues [17]. Briefly, 5×10^5 cells were collected, washed in PBS and pelleted. The pellet was resuspended in 400 ml of hypotonic buffer (20 mM HEPES pH = 7.9, 10 mM KCl, 0.1 mM ethylene diamine tetra acetic acid (EDTA), 0.1 mM EGTA, 1 mM dithiothreitol (DTT), 0.5 mM phenylmethyl sulphonyl fluoride (PMSF). The cells were allowed to swell on ice for 15 min. After which, 25 μl of an 18% solution of Nonie NF-40 was added, and the tubes were then vigorously vortexed for 10 s. The homogenate was centrifuged for 30 s in a microfuge. The nuclear pellet was resuspended in 50 μl of ice-cold buffer (20 mM HEPES pH = 7.9, 0.4 M NaCl, 1 mM EDTA, 1 mM EGTA, 1 mM DTT, 1 mM PMSF) and the tubes vigorously rocked at 4 °C for 15 min. Nucleic extracts were centrifuged for 5 min in a microfuge at 4 °C and the supernatant is frozen as aliquots at −70 °C. Of each cell treatment, 1–3 mg were incubated on ice for 30 min in 15 ml of buffer containing 10 mM TRIS pH = 7.5, 50 mM NaCl, 1 mM EDTA, 1 mM DTT, 3 mg poly (dI-dC), 2 ml of pab65 (Santa Cruz Biotechnology, INC), or non-specific antibodies, I ng of ^{32}[P]-end labelled oligonucleotide, part of the enhancer sequence from the HIV long terminal repeat (LTR) region (ENH7 from −115 to −81: GCTTGCTACAAGGGACTTTCCGCTGGGGACTTTCC) was added for another 15 min at room temperature. DNA-protein complexes were separated by electrophoresis through 5% native polyacrylamide gels, dried and visualised.

3. Results

We have previously reported that TNF potentiates the cytotoxicity induced by CPT, when incubated simultaneously, enhancing the induction of DNA- single strand breaks (SSB) in the human ovarian cancer cell line A2780 [9]. Although A2780 cells are sensitive to TNF-induced cytotoxicity in standard 3-(4,5-dimethylthiazol-2-yl)-2,5-diphenyltetrazolium bromide (MTT) assay (incubation time for 24 h with different concentrations of rHuTNF), cells are not sensitive (clonogenic assay) when treated for only 1 h. The cell survival fraction, after treatment with 1000 U/ml of rHuTNF, was ≅96%. Under the same experimental conditions, the IC_{50} of CPT alone was = 0.2 ± 0.08 μM and in combination with 1000 U/ml of rHuTNF was = 0.012 ± 0.03 μM with a potentiation rate of ≅16.7. The statistically significant CI was equal to 0.098 [95% CI = 0.042–0.261]. This finding strongly supports previous results [9,18] showing that TNF is able to potentiate CPT cytotoxicity.

The target of CPT is DNA Top I [8]. Top I is involved in DNA replication, transcription and recombination and in chromosome condensation and decondensation (recently reviewed in Ref. [8]). CPT reversibly stabilises the enzyme cleavage-complexes resulting in the generation of SSB. These SSB are reversible, but can be converted into lethal DSB during S phase, when the replication forks collides with the cleavable-complex [8,19]. According to these observations, cell cycle response of A2780 cells was examined 24 h after drug removal. Cells were treated for 1 h with CPT 0.2 μM alone, rHuTNF 1000 U/ml alone, or with CPT 0.012 μM + rHuTNF 1000 U/ml in combination and then incubated in drug-free medium for 24 h. Fig. 1 shows that TNF alone induces G_2-M (27.3 ± 1.1%) arrest (Fig. 1, panel B) while CPT treatment induces a strong S arrest (65.4 ± 1.8%) and a small fraction of sub-G_0–G_1 population (6.3 ± 0.8%) (Fig. 1, panel C). The combination CPT + TNF (Fig. 1, panel D) induces a very strong G_2-M arrest (44.2 ± 3.1%) and a fraction of sub-G_0–G_1 cell population (12.4 ± 2.8%) higher than that induced by CPT alone and a depletion of the S phase (12.5 ± 2.3%).

DNA synthesis was measured, at different times after drug removal, in cells exposed for 1 h to CPT 0.2 μM,

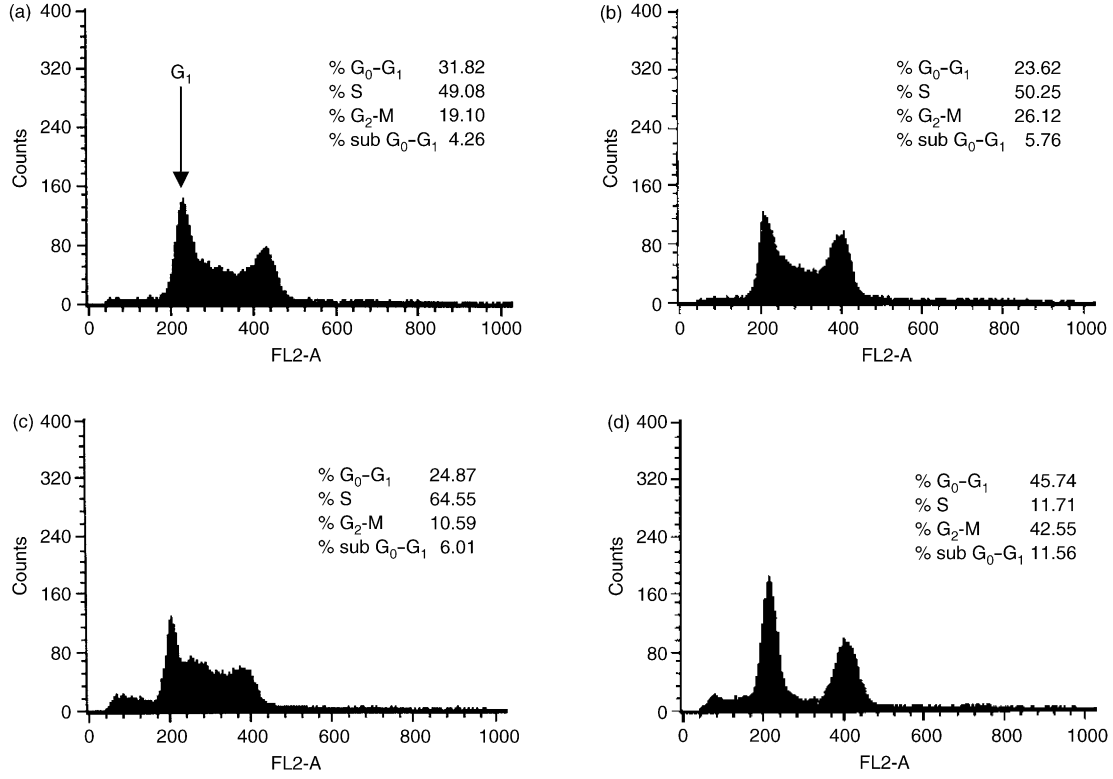

Fig. 1. Effects of TNF, CPT or CPT + TNF on cell cycle progression of A2780 cells. Cells were untreated (a), treated with rHuTNF 1000 U/ml (b), CPT 0.2 μM (c) or with CPT 0.012 μM + TNF 1000 U/ml (d) for 1 h and analysed by flow cytometry 24 h after drug removal. The figure is representative of three independent experiments, performed in duplicate.

rHuTNF 1000 U/ml or to a combination of both (CPT 0.012 μM + TNF 1000 U/ml) (Fig. 2). rHuTNF did not inhibit DNA synthesis. CPT inhibited it less profoundly than the combination, but for a longer period of time. The combination inhibited DNA synthesis for 1–2 h, with the DNA synthesis rate almost fully recovering 6–8 h after drug removal. DNA synthesis, in CPT-treated cells, recovered only to about 50% of the control level 8 h after drug removal.

The differential S-phase arrest (or depletion) induced by different treatments was investigated further by comparing the ability of A2780 cells to complete elongation of replicating DNA after CPT 0.2 μM alone, rHuTNF 1000 U/ml alone or CPT 0.012 μM + rHuTNF 1000 U/ml treatment. Pulse labelling with [^{3}H] thymidine and alkaline elution were used to study the state of newly-replicated DNA (Fig. 3). The longer the radio-labelled DNA fragment at the time of cell lysis, the slower the elution and the higher the fraction of labelled DNA remaining on the filter. Failure to elongate DNA leads to short radio-labelled DNA fragments, which are rapidly eluted. In the experiments shown in Fig. 3, the DNA was pulse labelled for 15 min with [^{3}H] thymidine immediately before a 1-h treatment, and elution was performed at various times after drug removal. In untreated cells (panel A), pulse-labelled DNA eluted with DNA fragments of increasing size with time, consistent with normal DNA replication and elongation (Fig. 3, panel A), similar slopes were observed in TNF-treated cells (Fig. 3, panel B). DNA elution at time 0 in the CPT-treated cells was faster than in the control cells (compare Fig. 3, panel C with panel A) and increased more in the CPT + TNF-treated cells (compare Fig. 3, panel D with panel C). This indicates that CPT and CPT + TNF can induce DNA breaks in newly-replicated DNA. However, DNA elongation in the CPT + TNF treated cells could be followed easily, and the DNA fragment length was approximately 90% of controls at 6 h, despite the massive induction of breaks seen at zero time (Fig. 3 panel D) In contrast, in the case of treatment with CPT alone even at 6 h after CPT removal, 88% of the DNA eluted faster than in the untreated cells (Fig. 3 panel C). These results indicate that the S-phase block observed in CPT-treated cells by flow cytometry is associated with a deficiency to complete DNA replication. In contrast, in the CPT + TNF-treated cells, DNA replication is completed 3–6 h after drug removal.

It was recently reported that the generation of DSB, but not SSB, is necessary for efficient NF-κB activation by CPT treatment [3,20]. These data imply that this activation pathway would be cell cycle coupled and may occur during the S-phase of the cell cycle [3,20]. The kinetics of the formation and persistence of the NF-κB

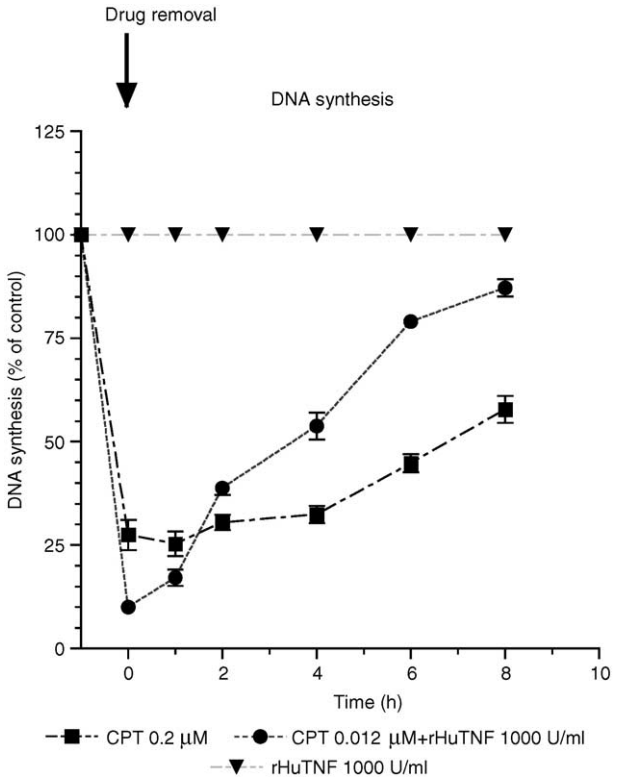

Fig. 2. Kinetics of DNA synthesis inhibition in A2780 cells. Cells were treated for 1 h and analysed by 10-min pulses with 1 μCi/ml [methyl-^{3}H] thymidine (80.9 Ci/mmol) followed by trichloroacetic acid (TCA) precipitation at different times after drug removal. Mean ± standard error of the mean (S.E.M.) of two independent experiments performed in duplicate.

complexes was further explored by EMSA. rHuTNF at 1000 U/ml, according to previous results [4,7], induced NF-κB complexes after a short treatment time; they were evident after 30 min of incubation in our study (Fig. 4a, lanes 6,7). CPT 0.2 μM did not induce NF-κB complexes until after 3 h treatment (Fig. 5, lane 3). The combination CPT 0.012 μM + rHuTNF 1000 U/ml also induced activation of NF-κB complexes but this was less pronounced than with TNF treatment alone (Fig. 4a, lanes 8–10).

The generation of the NF-κB complexes was also analysed in cells treated for 24 h. Looking at the persistence of the NF-κB complexes, it appears that they remained for 24 h in the TNF-treated cells (Fig. 4b, lane 4). In contrast, they were present for only 6 h (Fig. 4b, lane 6, Fig. 5, lane 4) and disappeared after 24 h in CPT-treated cells (Fig. 4b, lane 7, Fig. 5, lane 5). In the CPT + TNF-treated cells (Fig. 4b, lanes 8–10) NF-κB complexes, clearly visible after 1 h (lane 8), disappeared quickly, becoming undetectable at 6 h (lane 9).

Recent studies demonstrated that NF-κB activation by CPT could provide an anti-apoptotic function [3,6]. Since FACS analysis (Fig. 1) revealed a tendency of the combination CPT + TNF to induce apoptosis, a detailed analysis of DNA secondary fragmentation (apoptosis-associated) was evaluated by means of a FBA. We have previously shown [7] that rHuTNF alone, at a 1000 U/ml concentration, induced a small fraction of DNA-secondary fragmentation in a time-dependent manner when incubated for a long time (maximum effect after 48 h of continuous incubation). In these experiments, A2780 cells were treated for 1 h and processed at different times after drug removal. rHuTNF (1000 U/ml) did not induce any significant amount of DNA-secondary fragmentation (≅7.5%). CPT alone induced DNA-secondary fragmentation in a dose- and time-dependent manner (Fig. 6 panels a–d). The fragmentation started to appear at concentrations equal to 1.0 μM after 6 h and rose to a maximum after 24 h; 0.1 μM induced more than 25% of DNA fragmentation (as a% of the controls). In the presence of rHuTNF (1000 U/ml), the amount of DNA secondary fragmentation was higher than in the cells treated with CPT alone, it started immediately after 3 h and increased after 6 and 12 h, also in the presence of very low concentrations of CPT (0.01 and 0. 1 μM). After 24 h, the effect was maximal (Fig. 6 panels a and b). It is evident that the induction of DNA fragmentation is more severe following treatment with the combination CPT + rHuTNF than following CPT or rHuTNF alone.

The ApopTag assay confirmed the substantial induction of apoptosis. This was observed by the appearance of a dark brown colour in the nuclei, when cells were treated with 0.012 μM CPT in combination with 1000 U/ml of rHuTNF for 1 h and stained after 24 h incubation in drug-free medium [% of positive cells = 63.8 ± 3.2 ($P < 0.002$)] (Fig. 7). Apoptosis was induced in a small population of the control cells (2.4 ± 0.8), the cells treated with 0.2 μM of CPT (17.2 ± 2.3, non-significant) and the cells exposed to 1000 U/ml rHuTNF (5.6 ± 1.8, non-significant) (Fig. 7).

4. Discussion

In this report, we show that TNF sensitised A2780 cells to CPT-induced cytotoxicity. We demonstrated that the induction of apoptosis induced by TNF in combination with CPT is principally related to NF-κB inhibition in A2780 cells. Our observations also suggested that a shorter timescale in the appearance of NF-κB complexes in the combined treatment group is related to the ability of A2780 cells to undergo apoptosis.

In general, NF-κB most frequently exists as a heterodimeric complex between the p50 and p65 subunits. Nevertheless, the mammalian NF-κB/Rel family of proteins has five members, namely Rel (c-Rel), p65 (Rel A), Rel B, p50 (NFKB1) and p52 (NFKB2) [1,2] which can form heterodimers with one another. Activation of NF-κB is controlled by phosphorylation and proteolysis of an inhibitory subunit called IκB. Activation of

NF-κB is assumed to induce the transcription of genes that encode gene products that function to block apoptosis. Consistent with this hypothesis, the gene products of TRAF-1 and 2 and c-IAP1 and 2 are upregulated by NF-κB at the mRNA level and block the ability of TNF or other drugs (such as etoposide) to activate the caspases.

It has been shown that inhibition of NF-κB through the adenoviral delivery of a modified form of IκBα, the inhibitor of NF-κB, sensitises chemoresistant tumours to the apoptotic activities of TNF and CPT-11, resulting in tumour regression [6,21].

Rel A transactivation can also be regulated by the cyclin-dependent kinase inhibitor, $p21^{waf-1}$. As a consequence, p53 could indirectly stimulate NF-κB activity. However, p53 and NF-κB play divergent roles: activation of NF-κB is associated with the resistance to apoptosis (promoting cell survival), while p53 plays an important role in cell cycle arrest or apoptosis in response to various types of cellular stress [1,2].

The ubiquitin-proteasome pathway (specifically the 26S proteasome) is the principle mechanism by which cellular proteins, including ubiquitinated IκB, are degraded [22]. Inhibition of the ubiquitin-proteasome

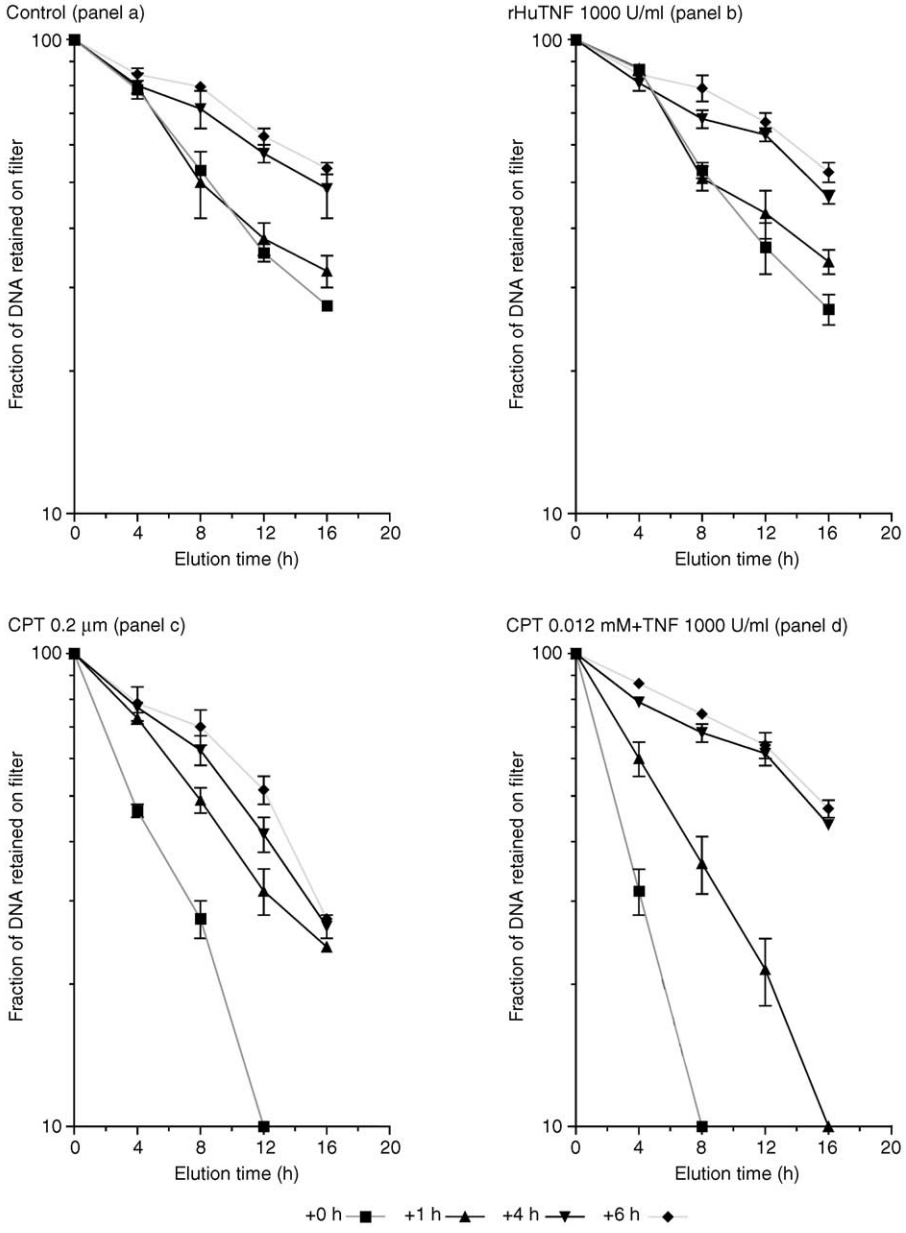

Fig. 3. Effects of TNF, CPT or CPT + TNF on DNA elongation in A2780 cells. Cells were untreated (a), treated with rHuTNF 1000 U/ml (b), CPT 0.2 μM (c) or with CPT 0.012 μM + TNF 1000 U/ml (d) for 1 h and analysed by pulse-labelling DNA elution at the indicated time after drug removal. Mean ± S.E.M. of two independent experiments performed in duplicate.

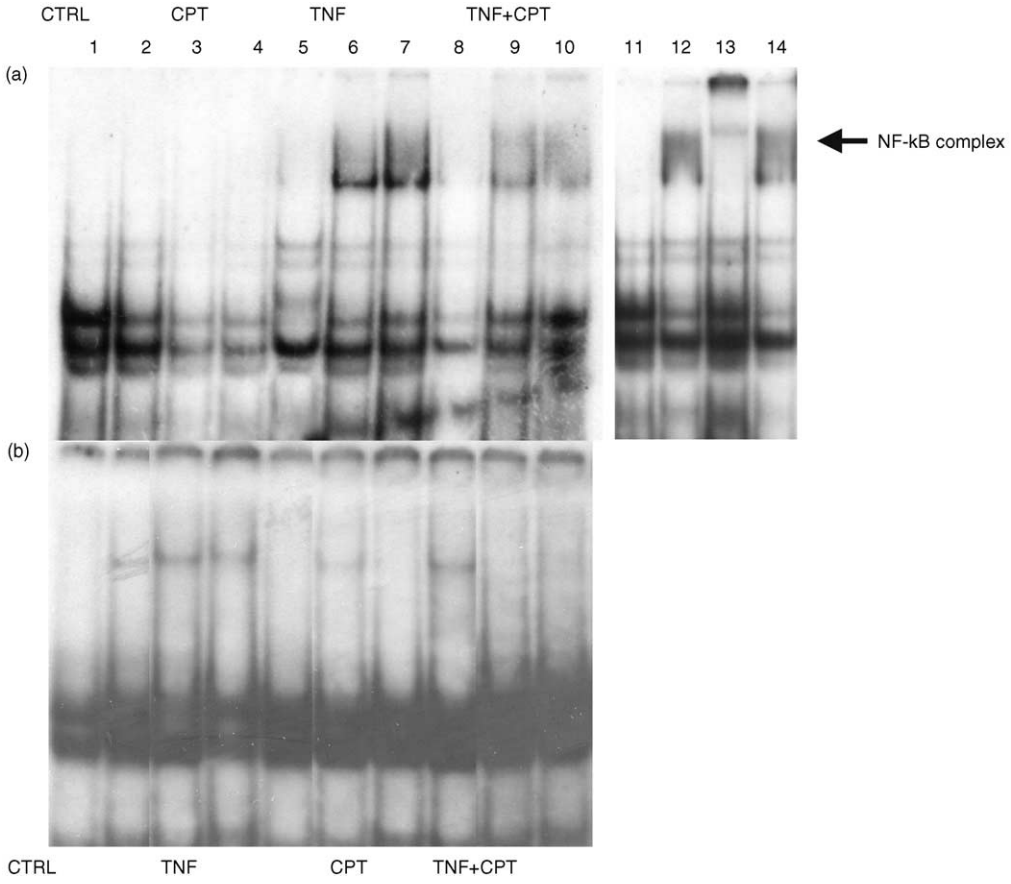

Fig. 4. Gel mobility shift analysis (EMSA) of NF-κB complexes. The figure is representative of three independent experiments. Nucleic extracts of A2780 cells, which were treated with different drugs for different times, were incubated with a labelled probe containing a NF-κB site and in the indicated lanes with the relevant antibodies. The position of the NF-κB complex is indicated by the right arrow. (Panel a) Gel shift assay with extracts from A2780 cells treated for short time. Lane 1: control; lanes 2–4: treated with CPT 0.2 μM analysed after 15 min (lane 2), 30 min (lane 3) and 1 h (lane 4); lanes 5–7: treated with rHuTNF 1000 U/ml analysed after 15 min (lane 5), 30 min (lane 6) and 1 h (lane 7); lanes 8–10: treated with CPT 0.012 μM + TNF 1000 U/ml analysed after 15 min (lane 8), 30 min (lane 9) and 1 h (lane 10). Lanes 11–14: extracts from A2780 cells with specific and unspecific antibodies after 30 min of rHuTNF 1000 U/ml treatment (lane 11: control, lane 12: TNF, lane 13: TNF + a/b p65, lane 14 TNF + a/b nsp). (Panel b) Cells were treated as reported above, but EMSA analysis was performed at different times after long-term drug exposure (from 1 h to 24 h). Lane 1: control; lanes 2–4: treated with rHuTNF 1000 U/ml analysed after 1 h (lane 2), 6 h (lane 3) and 24 h (lane 24); lanes 5–7: treated with CPT 0.2 μM analysed after 1 h (lane 5), 6 h (lane 6) and 24 h (lane 7); lanes 8–10: treated with CPT 0.012 μM + TNF 1000 U/ml analysed after 1 h (lane 8), 6 h (lane 9) and 24 h (lane 10).

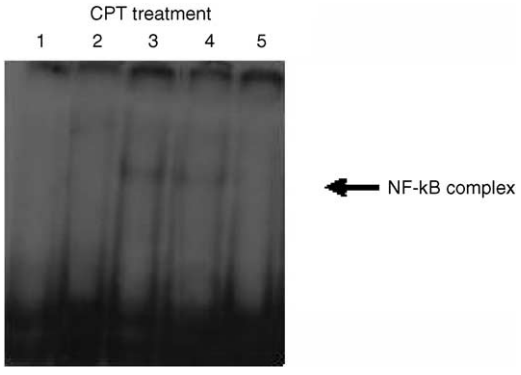

Fig. 5. Gel mobility shift analysis of NF-κB complexes. The figure is representative of three independent experiments. Gel shift assay with extracts from A2780 cells treated with CPT 0.2 μM for long periods of time. Lane 1: control; lanes 2–4: treated with CPT 0.2 μM analysed after 1 (lane 2), 3 h (lane 3), 6 h (lane 4) and 24 h (lane 5).

pathway results in the deregulation of cellular proteins involved in cell cycle control, the promotion of tumour growth, and induction of apoptosis [22]. The proteasome inhibitor, PS-341 (dipeptide boronic acid analogue), has been shown to block NF-κB activation through stabilisation of IκB [2]. Pretreatment of cancer cells with PS-341, prior to exposure to SN-38 (the active metabolite of CPT-11), potently increases the growth inhibition effect induced by SN38 through a massive induction of apoptosis [23].

Thus, NF-κB activation serves as a principal mechanism for inducible resistance to chemotherapy.

CPT causes the formation of SSB by top I, but collision between the nicked DNA top I complex and a DNA replication fork leads to a DSB. Aphidicolin prevents S-phase-specific toxicity of CPT and diminishes NF-κB activation by CPT, but not by etoposide [3,20].

Etoposide is a Topoisomerase II (top II) inhibitor. Top II creates transient DSB, which are necessary for DNA replication and division [24]. This suggests that DSB are necessary for NF-κB activation. These data also imply that this activation pathway may occur only in the S phase of the cell cycle.

Pulse-labelling alkaline elution experiments in this study indicated that both CPT and CPT + TNF treatment can induce DNA breaks in newly-replicated DNA. However, DNA elongation in the CPT + TNF treated cells revealed that approximately 90% of DNA, at six hours after drug removal, eluted in a similar manner to the controls. In contrast, in the case of treatment with CPT alone, even at 6 h after CPT removal, 88% of the DNA eluted faster than in the untreated cells. These results indicate that the S-phase block observed in CPT-treated cells, by flow cytometry and in the DNA synthesis experiments, is associated with a deficiency to complete DNA replication. In contrast, in CPT + TNF-treated cells the DNA replication is completed 3–6 h after drug removal. At six hours after drug removal, NF-κB complexes were not detectable in cells treated with the

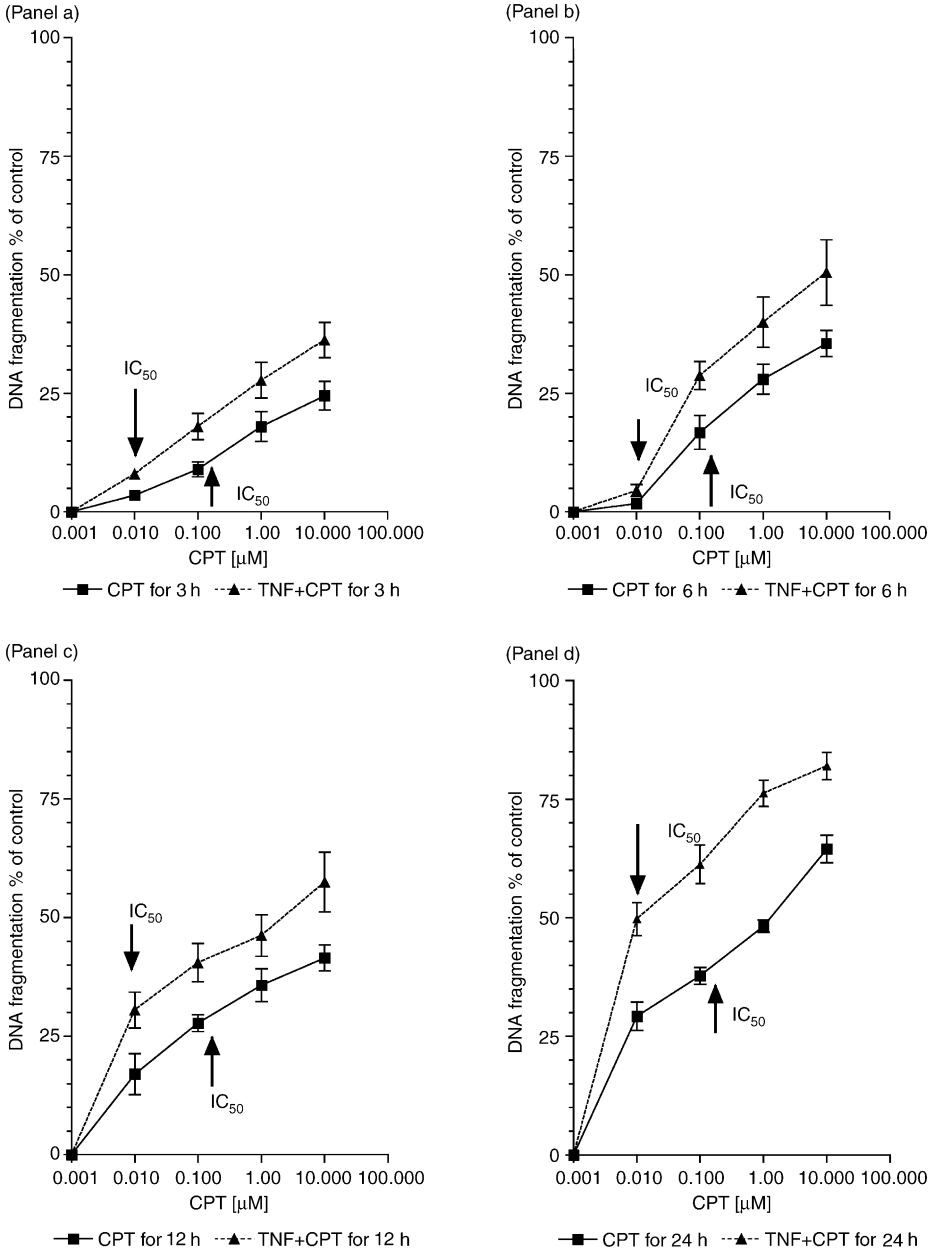

Fig. 6. Induction of DNA secondary fragmentation (apoptosis-related), evaluated by a filter binding assay (FBA) induced by CPT 0.2 μM or CPT 0.012 μM + TNF 1000 U/ml. Cells were treated for 1 h and then incubated in drug-free medium for different times. Panel a after 3 h, panel b after 6 h, panel c after 12 h and panel d after 24 h. Each point represents the mean ± S.E.M. of at least 3 independent experiments performed in duplicate.

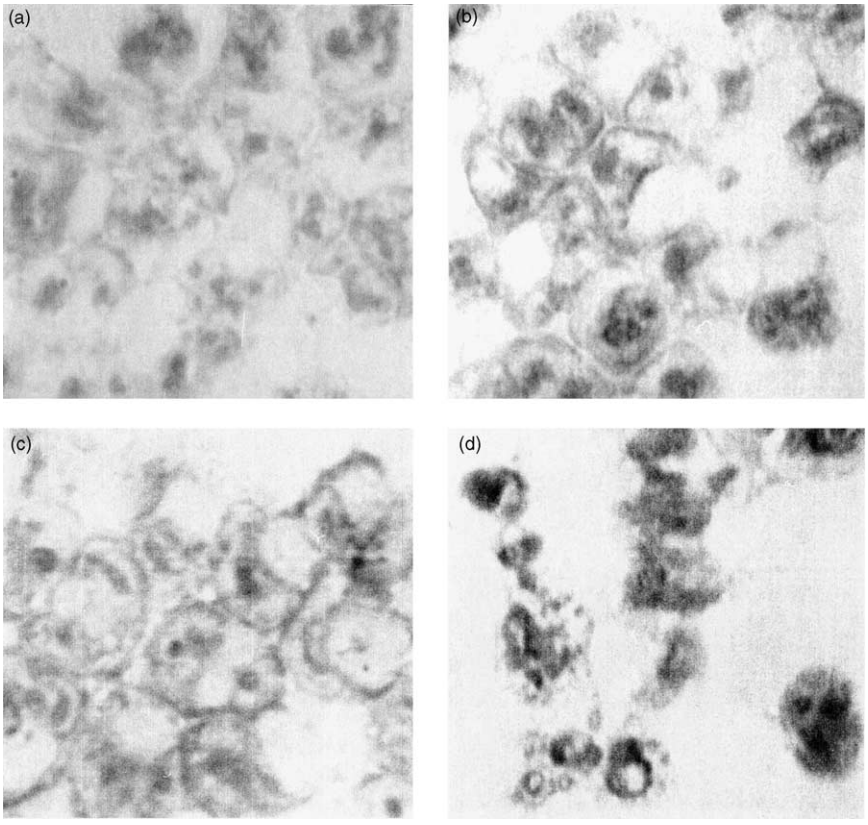

Fig. 7. Detection of apoptosis by ApopTag staining (representative figure from independent experiments) of A2780 cells untreated (a) or treated for 1 h with CPT 0.2 μM (b), TN F1000 U/ml with (c) or CPT 0.012 μM + TNF 1000 U/ml (d) and stained after 24 h incubation in drug-free medium. The nuclei of apoptotic cells were stained dark-brown.

combination, while they persisted in cells treated with CPT alone. These data imply that NF-κB activation in A2780 cells cannot occur when DNA replication is completed.

In conclusion, our findings show that TNF, administered simultaneously with CPT, reduces the time that NF-κB complexes persist in the cells, causing induction of apoptosis and, consequently, a strong synergistic cytotoxic effect.

CPT derivatives, such as irinotecan (Camptosar) and topotecan (Hycamptin) are approved by the Food and Drug Administration (FDA) in the United States; several analogues are in various stages of clinical evaluation (i.e. 9-aminocamptotecin and rubitecan). Topotecan is currently utilised in second-line therapy for advanced ovarian cancer [25].

In previous phase I and II studies, it has been demonstrated that intraperitoneal rHuTNF has a high degree of efficacy in reducing or eliminating ascitic fluid [26,27].

In cancers limited to the abdominal cavity, the intraperitoneal administration of antineoplastic drugs could be the treatment of choice because of both the limited systemic toxicity and the pharmacokinetic advantages. We have previously shown that weekly intraperitoneal administration of mitoxantrone (6 mg/m^2) and TNF (200 μg/m^2) is a feasible regimen with acceptable toxicity [27].

Thus, the possibility to use TNF in combination with CPT derivatives may represent an alternative therapy for relapsed cancer patients.

Acknowledgements

The technical assistance of Dr Guido Cimoli in performing the ApopTag experiments and of Dr Faina Vikhanskaya (Laboratory Experimental Oncology, Genova, Italy) in performing the EMSA experiments was very much appreciated. This work was partially supported by the TENDER No. 2000/S 118-076796 "Induction of conformational changes in p53 mutants and modulation of sensitivity to selective anti-cancer drugs", awarded by the European Community, Ispra (Varese), Italy (2003) to PR.

References

1. Barkett M, Gilmore TD. Control of apoptosis by Rel/NF-kB transcription factor. *Oncogene* 1999, **18**, 6910–6924.
2. Mayo MW, Baldwin AS. The transcription factor NF-kappaB:

control of oncogenesis and cancer therapy resistance. *Biochim Biophys Acta* 2000, **270**, M55–M62.
3. Huang TT, Wuerzberger-Davis SM, Seufzer J, *et al*. NF-kB activation by Camptothecin. *J Biochem Chem* 2000, **275**, 9501–9509.
4. Rath PC, Aggarwal BB. TNF-induced signaling in apoptosis. *J Clin Immunol* 1999, **19**, 350–364.
5. Schmitt CA, Lowe SW. Apoptosis and therapy. *J Pathol* 1999, **187**, 127–137.
6. Wang C-Y, Cusack JC, Liu R, Baldwin AS. Control of inducible chemoresistance: enhanced anti-tumor therapy through increased apoptosis by inhibition of NF-κB. *Nature Med* 1999, **5**, 412–417.
7. Vikhanskaya F, Falugi C, Valente P, Russo P. Human papillomavirus type 16 E6-enhanced susceptibility to apoptosis induced by TNF in A2780 human ovarian cancer cell line. *Int J Cancer* 2002, **97**, 732–739.
8. Pourquier P, Pommier Y. TopoisomeraseI-mediated DNA damage. *Adv Cancer Res* 2001, **80**, 189–216.
9. Orengo G, Noviello E, Cimoli G, *et al*. Potentiation of Topoisomerase I and II inhibitors cell killing by Tumor Necrosis Factor: relationship to DNA strand breakage formation. *Jpn J Cancer Res* 1992, **83**, 1132–1136.
10. Valenti M, Cimoli G, Parodi S, *et al*. Potentiation of Tumor Necrosis Factor-mediated cell killing by VP16 on human ovarian cancer cell lines [''in vitro'' results and clinical implications]. *Eur J Cancer* 1993, **29A**, 1157–1161.
11. Chou T-C, Talalay P. Generalized equations for the analysis of inhibitors of Michaelis-Menten and higher order kinetic systems with two or more mutually exclusive and nonexclusive inhibitors. *Eur J Biochem* 1981, **115**, 207–216.
12. Chou T-C, Talalay P. A simple generalized equation for the analysis of multipleinhibitions of Michaelis-Menten kinetic systems. *J Biol Chem* 1987, **252**, 6438–6442.
13. Debernardis D, Stanzione S, Ottoboni C, *et al*. Endogenous TNF enhances Topoisomerase II inhibitors activity in human ovarian cancer cell lines. *J Pharmacol Exper Ther* 1996, **279**, 84–90.
14. Covey JM, D'Incalci M, Tilchen EJ, Zaharko DS, Kohn KW. Differences in DNA damage produced by incorporation of 5-Aza-2′-deoxycitidine or 5,6-dihydro-5-azacytidine into DNA of mammalian cells. *Cancer Res* 1986, **46**, 5511–5517.
15. Russo P, Poggi L, Parodi S, Pedrini AM, Kohn KW, Pommier Y. Production of protein-associated DNA breaks by 8-methoxycaffeine, caffeine and 8-chlorocaffeine in isolated nuclei from L1210 cells: comparison with those produced by Topoisomerase II inhibitors. *Carcinogenesis* 1991, **12**, 1781–1790.
16. Bertrand R, Pommier Y. Assessment of DNA damage in mammalian cells by filter elution methodology in cell growth and apoptosis: a pratical approach. In Studzinski GP, ed. *DNA Damage*. Oxford, University Press, 1996, 97–117.
17. Shreiber E, Matthias P, Muller MM, Schaffner W. Rapid detection of octamer binding proteins with ''mini-extracts'', prepared from a small number of cell. *Nuc Acids Res* 1989, **15**, 6419–6421.
18. Utsugi T, Mattern MR, Mirabelli CK, Hanna N. Potentiation of topoisomerase inhibitor-induced DNA strand breakage and cytotoxicity by tumor necrosis factor: enhancement of topoisomerase activity as a mechanism of potentiaton. *Cancer Res* 1990, **50**, 2636–2640.
19. Strumberg D, Pilon AA, Smith M, Hickey R, Malkas L, Pommier Y. Conversion of topoisomerase I cleavage complexes on the leading strand of ribosomal DNA into 5′-phosphorylated DNA double-strand breaks by replication runoff. *Mol Cell Biol* 2000, **20**, 3977–3987.
20. Piret B, Piette J. Topoisomerase poisons activate the transcription factor NF-kappaB in ACH-2 and CEM cells. *Nuc Acid Res* 1996, **24**, 4242–4248.
21. Wang C-Y, Mayo MW, Komeluk RG, Goeddel DV, Baldwin AS. NF-κB antiapoptosis: induction of TRAF-1, TRAF-2, c-IAP1 and c-IAP-2 to suppress caspase-8 activation. *Science* 1998, **281**, 1680–1683.
22. Elliott PJ, Adams J. Recent advances in understanding proteasome function. *Curr Opin Drug Discovery Dev* 1999, **2**, 484–490.
23. Cusack Jr. Jc, Liu R, Houston M, *et al*. Enhanced chemosensitivity to CPT-11 with proteasome inhibitor PS-341: implications for systematic nuclear factor-kappaB Inhibition 1. *Cancer Res* 2000, **61**, 3535–3540.
24. Champoux JJ. DNA topoisomerases: structure, function, and mechanism. *Ann Rev Biochem* 2001, **70**, 369–413.
25. Garcia-Carbonero R, Supko JG. Current perspectives on the clinical experience, pharmacology, and continued development of the camptothecins. *Clin Cancer Res* 2002, **8**, 641–661.
26. Hirte HW, Miller D, Tonkin K, *et al*. A randomized trial of paracentesis plus intraperitoneal tumor necrosis factor-alpha versus paracentesis alone in patients with symptomatic ascites from recurrent ovarian carcinoma. *Gynecol Oncol* 1997, **64**, 80–87.
27. Del Mastro L, Venturini M, Giannessi PG, *et al*. Intraperitoneal infusion of recombinant human tumor necrosis factor and mitoxantrone in neoplastic ascites: a feasibility study. *Anticancer Res* 1995, **15**, 2207–2212.